PHYSICAL REVIEW A VOLUME 10, NUMBER 2 AUGUST 1974

Small-angle scattering in stripping collisions of hydrogen atoms having energies of 1–10 keV in various gases*

H. H. Fleischmann
School of Applied and Engineering Physics, and Laboratory for Plasma Studies, Cornell University, Ithaca, New York 14850

C. F. Barnett and J. A. Ray
Thermonuclear Division, Oak Ridge National Laboratory, Oak Ridge, Tennessee 37830
(Received 7 May 1973; revised manuscript received 11 February 1974)

Angular distributions of protons resulting from stripping collisions of neutral hydrogen atoms in the ground state with He, Ar, Kr, H_2, N_2, O_2, H_2O, CO_2, and C_6H_6 have been measured for beam energies E between 1–10 keV and angles of up to 7°. They are found to be strongly peaked in forward direction. Where known, total stripping cross sections were used to derive absolute differential cross sections $d\sigma/d\Omega$. For a given gas, the distribution widths vary roughly proportional to $1/E$. The product of beam energy and the half-cone angle θ_{50} into which 50% of all protons are scattered varies from approximately 0.5 keV deg for H_2 to approximately 1.7 keV deg for Kr and C_6H_6. For the atomic target gases, deduced normalized differential cross sections $\rho = \theta \sin\theta \, d\sigma/d\Omega$ as functions of $E\theta$ agree in shape roughly with those derived for elastic scattering of hydrogen atoms. The impact parameters corresponding to θ_{50} are estimated. The significance of the peaking in forward direction is investigated.

I. INTRODUCTION

Over the last 20 years, extensive efforts have been made in the experimental and theoretical investigations of collisions between atomic and/or molecular particles. From these investigations, commensurate understanding has evolved or is presently being developed for charge-transfer reactions, inner-shell excitations, and also curve-crossing effects. However, comparatively little knowledge still exists on the stripping of outer electrons, in particular, for collisions between heavy atoms or ions. In this area, extensive experimental material on total cross sections for collisional electron losses has been collected by many groups.[1] But, reliable theoretical calculations still are limited to collisions involving only the lightest atomic particles H and/or He. For collisions involving heavier particles, theoretical calculations based on the statistical Thomas-Fermi model of atoms have been made[2,3] assuming a statistical "heating" of the electron gas and subsequent "evaporation" of one or more electrons. From this base, Firsov[3] arrives at a general scaling law for energy dependence and absolute values of the total electron-loss cross sections for collisions between atomic particles of comparable mass. These predictions seem to describe reasonably well electron losses in a number of collisions between rare-gas atoms, and therefore, are relatively widely accepted and quoted. However, a more recent analysis[4] of a wider range of experimental data revealed significant deviations in many other cases of single-electron-loss collisions. The cross sections for the deviating collisions seemed to be described better by an empirical scaling law more relevant to direct "knock-on" transitions of an electron from the bound state into the continuum. One consequence of this lack of understanding of these reactions can be seen in the fact that so far only rather few detailed measurements of the angular scattering of the resulting stripped particles have been published, compared with the large material on total cross sections. For electron-loss collisions involving heavy atomic particles, small-angle measurements have been published by Kaminker and Fedorenko[5] for the case $Ar^+ + Ar$, and more recently, by Savola *et al.*[6] and Francois[7] for helium projectiles on various gases. Further measurements, generally involving somewhat deeper penetration of the respective electron shells, have been performed by the Connecticut group.[8] Also, a limited number of groups[9,10] measuring total cross sections have made checks and published respective data on percentages of resulting particles scattered into various small cone angles. However, a large number of papers dealing with total cross sections do not show any investigations of the scattering connected with these reactions, and thus, may contain systematic errors resulting from this effect which can be estimated only when more scattering data become available. Furthermore, data on the scattering in stripping collisions, in particular of hydrogen atoms, are often needed in diagnostic measurements of neutral hydrogen atoms emerging from confined plasmas.

The present paper is addressed to this point and reports on some measurements of small-angle distributions of protons resulting from stripping

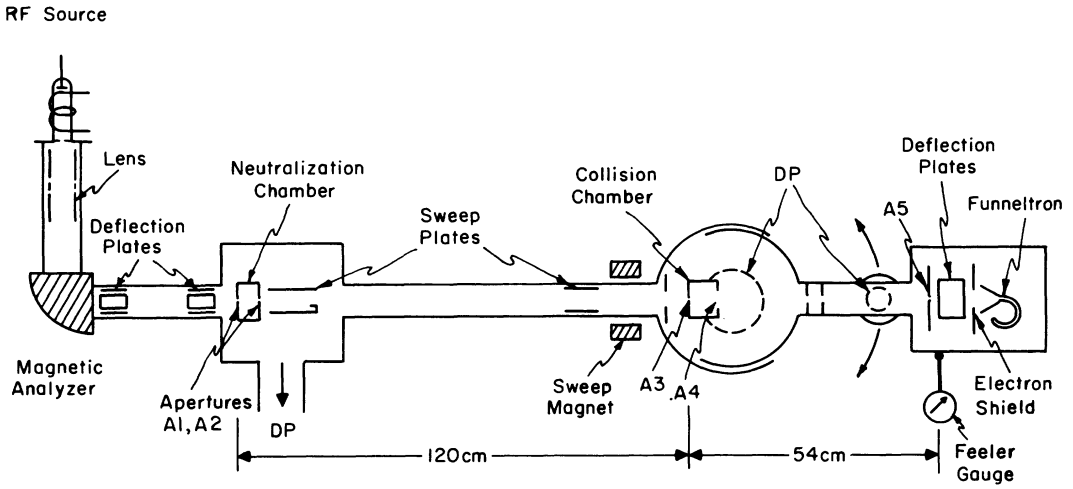

FIG. 1. Schematic diagram of experimental arrangement.

collisions of neutral hydrogen atoms in the ground state having kinetic energies E between 1 and 10 keV in He, Ar, Kr, H_2, N_2, O_2, H_2O, CO_2, and C_6H_6. It is found that the width of these distributions varies roughly inversely with the beam energy for any given target gas. The product of the half-cone-angle θ_{50} into which 50% of the protons are scattered multiplied with the beam energy was observed to vary relatively little from $E\theta_{50} \approx 0.5$ keV deg for hydrogen to $E\theta_{50} \approx 1.7$ keV deg for Kr and C_6H_6. Where known, absolute total cross sections were used to derive absolute values for the differential cross sections $d\sigma/d\Omega$. The respective reduced differential cross sections $\rho = \theta \sin\theta \, d\sigma/d\Omega$ plotted as a function of $E\theta$ generally are similar for various beam energies for any given target gas. For the atomic target gases, they agree roughly with those derived for the elastic scattering of protons by these gases. It appears that some of the published data on total stripping cross sections of hydrogen atoms in these gases may have underestimated these scattering effects.

II. EXPERIMENTAL ARRANGEMENT

Most of the measurements were performed using the experimental setup shown in Fig. 1. H^+ ions were obtained from a rf ion source with H_2 gas fed through a Pd gas leak. Plasma probe potentials of 100 to 400 V were used to expell the ions through the exit aperture. Electric deflection measurements indicated ion energies corresponding to a birth potential within 20–30 V of this plasma electrode. After passing through an acceleration and focusing lens, the extracted ions were analyzed in a 90° deflection magnet.

After further directional corrections, the selected H^+ beam entered a charge-transfer cell, 2.5 cm long and 2 cm in diameter. For all measurements with beam energies at 2 keV or above, its entrance aperture was 1 mm in diameter. For measurements at 1 keV, this aperture had to be increased to 2 mm in diameter to obtain sufficient intensity. The exit aperture of the cell was 2 and 3 mm wide, respectively. The gas pressure in the cell was measured and monitored by a MKS capacitive pressure meter. Generally nitrogen at a few mTorr pressure was used in the experiment. With the gas feed closed, the background pressure in the cell was less than 10^{-5} Torr. After leaving the cell, the remaining ions were separated from the neutral beam and collected on a plate using electric deflection fields of about 500 V/cm, which also served to quench the metastable H(2s) atom component in the beam. An oil diffusion pump kept the pressure outside the neutralization cell below 10^{-6} Torr.

After a free-flight pass of 1.05 m, the neutral beam entered the collision chamber through an aperture 1 or 0.5 mm in diameter for beam energies $E = 1$ keV or $E \geq 2$ keV, respectively. Ions produced between the two gas cells were swept aside by another set of electric deflection plates and magnets in front of the collision chamber. The collision chamber itself was 2.5 cm long and 2 cm in diameter. The target-gas pressure was again measured and monitored using an MKS instrument. Generally, target pressures of a few times 10^{-4} Torr were used in the experiment. With the gas feed turned off, this pressure sank below 10^{-5}

Torr. The exit aperture consisted of a slit 4 mm high and 8 mm wide, thus permitting transmission of all particles scattered less than 8° in the horizontal direction and less than about 3°–4° in the vertical direction. All apertures were made from Mo foil 0.1 mm thick. The stripping cell was mounted in a vacuum chamber about 25 cm in diameter which was pumped by a diffusion pump, which kept the pressure in this larger chamber below a few times 10^{-6} Torr. An additional shield around the collision chamber prevented beam particles from bypassing the collision chamber.

A detector system for ions formed in stripping collisions of the neutral hydrogen atoms with the target was mounted on an arm which could be rotated around the center of this chamber. Its entrance aperture was positioned 54 cm from the center of the collision cell. To decrease the residual density of target gas directly in front of the detector, two 1.5-cm-wide apertures and a 2-in. diffusion pump were inserted in the movable arm. The angular position of this arm was determined by two oppositely positioned feeler gauges, permitting measurements for scattering angles of up to about 7°.

The ion detection system consisted of an entrance aperture, electric deflection plates for separation of the various charge states, and a Bendix funneltron electron multiplier. The entrance aperture consisted again of holes 0.5 mm and 1 mm wide for $E \geq 2$ keV and $E = 1$ keV, respectively, drilled in a 0.1-mm tungsten foil. This aperture was mounted on a sled which could be moved from the outside in the vertical direction. Also the deflector plates, 2.5 cm square and 1.8 cm apart, were mounted on the same sled. The funneltron having a sensitive area 10 mm in diameter was mounted on a second vertical sled which allowed it to be positioned either directly in the path of the scattered neutral atoms or up to 2 cm away from it, which was sufficient for a complete separation of ions from neutrals. For further suppression of unwanted signals, stemming from secondary electrons produced in the detection chamber by particles other than the wanted charge state, a small negatively charged shield was introduced in front of the funneltron. By these means, in the ion detection position, the detection efficiency for neutral atoms was reduced by a factor 10^{-5}, which made this effect negligible in all measurements.

The funneltron itself was operated in a charge-saturated mode, and the signals were counted after amplification and pulse shaping. Count rates generally varied from a few to 10^4 sec^{-1}. Thus, count losses either by pileup or by reductions in signal size were kept below a few percent and no corrections had to be applied to the final results. Non-beam-produced background from electronic noise and spurious pulses in the detector amounted to no more than a few pulses per minute.

III. PROCEDURES AND TESTS

After construction of the apparatus, an optical alignment of all apertures of the charge transfer cell, the collision chamber, and the detector arm was performed, and it was also checked periodically later. Particular attention was given to the position of the horizontal exit slit of the collision cell to ensure that the full beam length within the cell could be seen through the detector entrance aperture for all angular positions used in the following measurements.

Thereafter, at the beginning of each series of measurements, the detector arm was put in the forward position, the funneltron was moved into the center position to detect neutrals, and a small gas pressure was introduced into the neutralization cell. Then, the beam was tuned to maximize the pulse rate from the detector. When maximized, this rate generally was too high to allow pulse counting, and the detector output was directly observed on an oscilloscope. However, separate measurements were made with intentionally reduced ion-beam currents, using pulse

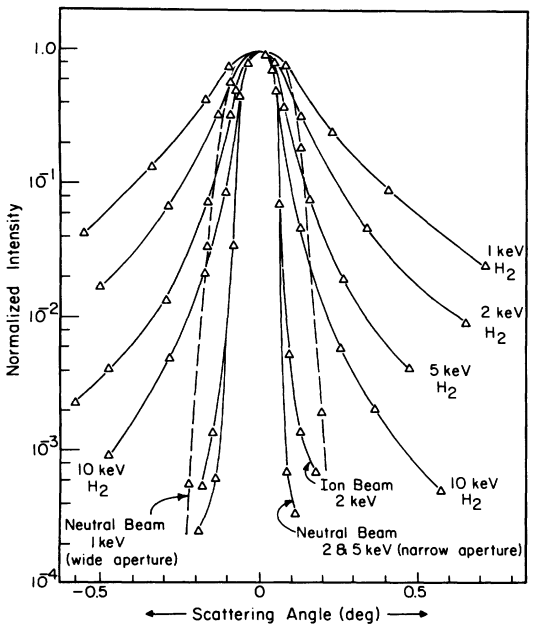

FIG. 2. Angular distributions of the neutral-atom beam using narrow and wide aperture sets and a direct ion beam using the narrow apertures. For comparison, small-angle distributions of protons from stripping collisions of neutral atoms in hydrogen are also shown.

counting to determine the angular resolution of the neutral-atom signals. Results for the two sets of apertures used are included in Fig. 2 and compared with some angular distributions of stripped protons. The width of these neutral-atom distributions agrees with that expected from the geometric conditions. Also, the position of the neutral beam in the detector plane coincided very well with the optical alignment.

Similar resolution measurements were made at $E = 2$ keV using the original ion beam. In this case, the funneltron was placed in the ion detection position, the ion beam was further detuned, the deflection fields between the neutralization cell and the collision cell were removed, and no gas was fed into either cell.

After determination of the vertical and horizontal positions of the ion-beam center, which was somewhat displaced from that of the neutral beam, the angular distribution of the ions was determined. The result is also included in Fig. 2, with the beam centers shifted into the same positions. It appears that the width of this ion beam was virtually identical with that of the neutral beam, in spite of its angular deflection, i.e., the remaining deflection fields, including the normal fields between collision cell and detector aperture, seem to have been of large scale and, thus, only to have deflected the beam as a whole but not to have changed its internal distribution.

In the normal experimental runs, the neutralization and target-gas pressures were adjusted after beam tuning. Within the detector, the funneltron was brought into the position for ion detection, and the horizontal and vertical position of the center of the stripped-ion distribution was determined. In general, this center was displaced from the original neutral beam by about 0.1°–0.2°, depending on the beam energy.

After a corresponding adjustment of the detector-sled positions, the detector arm was moved to one large-angle position and then stepwise moved through the ion-beam center to the opposite extreme position. At each step, pulses were counted for generally 10–40 sec, resulting in a total count of generally between 100 and 100 000 counts at the wings and the center of the distribution, respectively. The separation of the count positions was varied according to the steepness of the distribution. At various positions, the background rate was determined by shutting off the target gas and/or the neutralization gas or by shorting out the deflection voltage in the detector or some combinations thereof. In practically all cases, it was found that the total background contributions to the count rate amounted to less than 10%. During

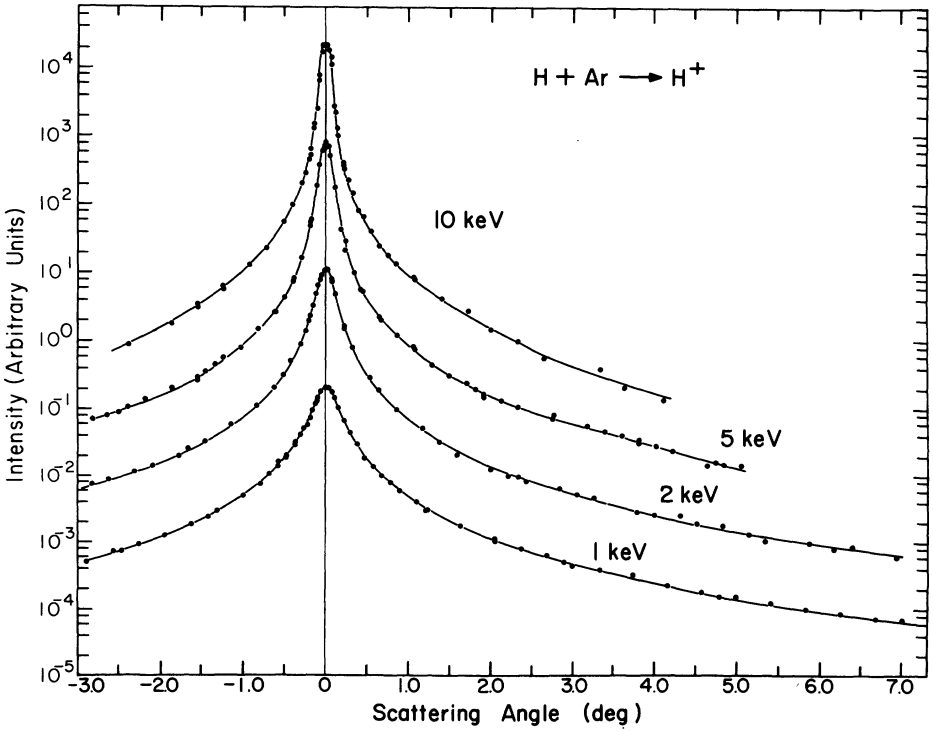

FIG. 3. Example of measured distributions for argon as target gas. (The curves are arbitrarily displaced in the vertical direction).

a run, the stability of the original ion-beam current and the various gas pressures was monitored. For consistency, the measured distribution was retraced at the end of each run moving the detector in a few larger steps opposite to the original direction, and the data were only accepted from runs in which the back tracing agreed to within about 10% with the initial data. An apparent shift of the beam center between the two directions of movement amounted to less than 0.01°.

During the actual data gathering phase, generally a number of runs with various target gases were done at any given beam energy. Both, in the initial test phase and also later, a number of acceptable runs were repeated, and the results were found to reproduce generally to better than 10%. Only at the steepest-curve parts deviations of up to 20% occurred.

In some cases where the difference of the count rates between the center and the wings of the distribution was too large, two runs at different target-gas pressures were measured: one "low-pressure" run [typically at $(1-2)\times10^{-4}$ Torr] in which the center of the distribution was emphasized, and one "high-pressure" run [typically at $(4-8)\times10^{-4}$ Torr] in which mainly the wings were investigated. The two measured distributions then were fitted together at intermediate angles at which both measurements were reliable.

An example of the distributions thus determined is shown in Fig. 3 for argon as target gas. (The vertical scales of the various distributions are displaced by arbitrary factors.) In these distributions, the left-right symmetry which mainly depends on the alignment of the target cell and the homogeneity of any incidental deflection fields between the target cell and the detector generally was preserved within the experimental fluctuations

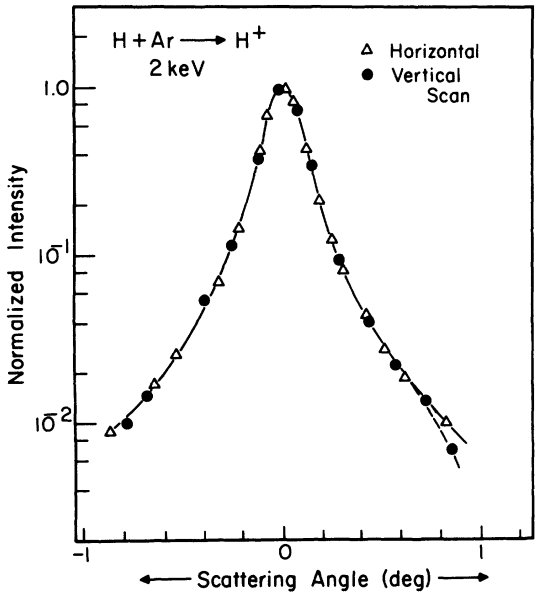

FIG. 4. Comparison of small-angle distributions for argon as target gas and 2-keV beam energy measured in the vertical and horizontal directions.

of about 10%, or about 0.01° in the steeper parts of the distributions. Larger asymmetries were observed only in cases of poor target-cell alignment.

To check the validity of these procedures and thus the reliability of the resulting distributions, a number of tests were performed after the assemblage of the apparatus and during the measurements.

The energy of the ions after acceleration was determined by measuring the magnetic deflection field in the mass analyzer. As mentioned, this energy corresponded to within about 20 eV to a

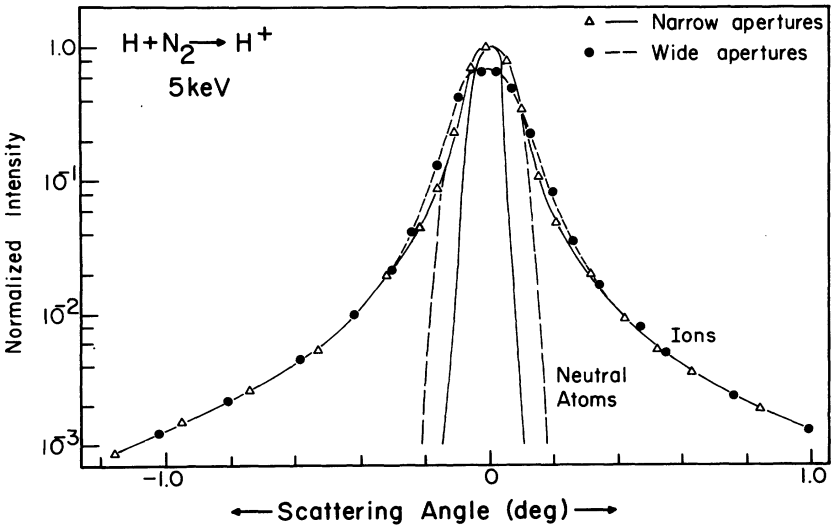

FIG. 5. Influence of beam resolution on measured distributions. Angular distributions for nitrogen at 5 keV measured with wide and narrow aperture sets and compared with neutral-beam curves.

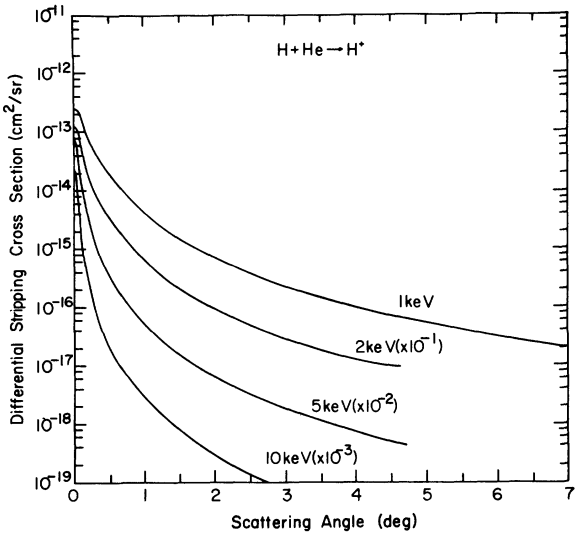

FIG. 6. Differential stripping cross sections for helium. Assumed total cross sections $\sigma_{01}=0.3\times10^{-16}$ cm^2 for 1 keV, 0.6×10^{-16} cm^2 for 2 keV, 1.2×10^{-16} cm^2 for 5 keV, and 1.4×10^{-16} cm^2 for 10 keV (Refs. 12 and 13). (See also Ref. 11.)

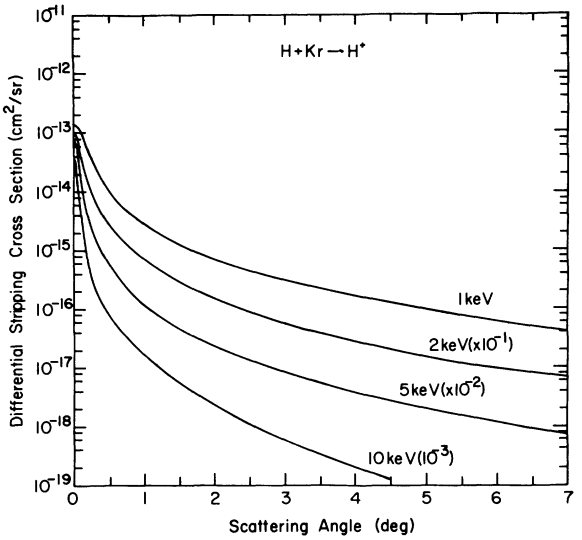

FIG. 8. Differential stripping cross section for krypton. Assumed total cross sections $\sigma_{01}=0.3\times10^{-16}$ cm^2 for 1 keV, 0.7×10^{-16} cm^2 for 2 keV, 1.55×10^{-16} cm^2 for 5 keV, and 3.0×10^{-16} cm^2 for 10 keV (Refs. 13 and 14). (See also Ref. 11.)

birth potential of the ions equal to the plasma probe in the rf source. This result was reconfirmed by electric deflection measurements and by comparative measurements with an electron-bombardment ion source. Therefore, in all measurements, the regulated accelerator voltage was connected to this plasma electrode and all beam energies are quoted this way.

The background count rate produced from effects other than charge transfer in the neutralization cell and subsequent ionization by collisions with the target gas have been tested as mentioned. Additional tests were performed to determine the signal contributions from ions produced in colli-

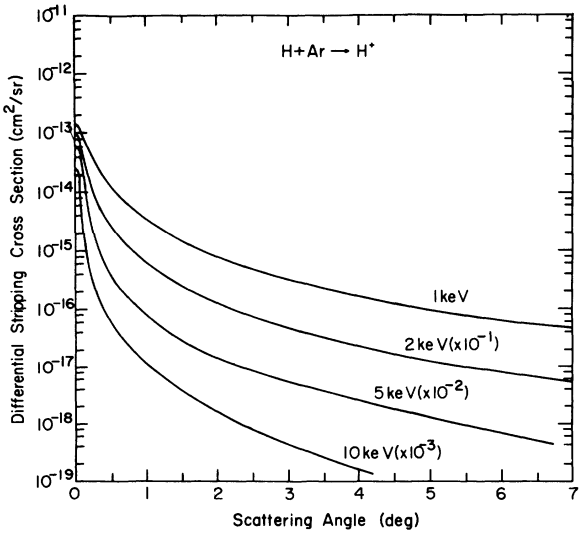

FIG. 7. Differential stripping cross sections for argon. Assumed total cross sections $\sigma_{01}=0.3\times10^{-16}$ cm^2 for 1 keV, 0.6×10^{-16} cm^2 for 2 keV, 1.3×10^{-16} cm^2 for 5 keV, and 2.1×10^{-16} cm^2 for 10 keV (Refs. 12, 13, and 14). (See also Ref. 11.)

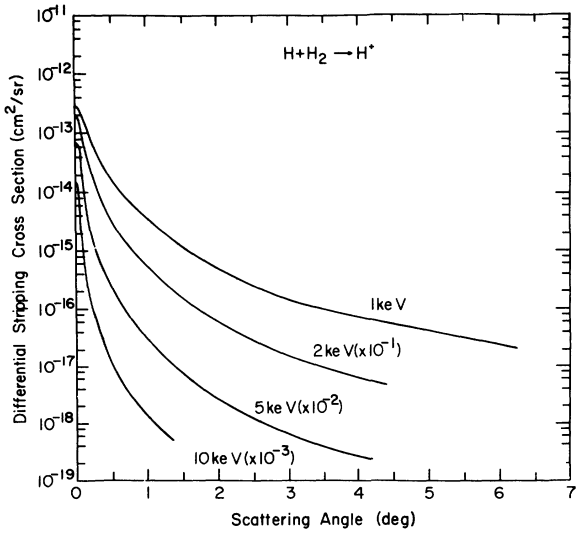

FIG. 9. Differential stripping cross sections for molecular hydrogen. Assumed total cross sections $\sigma_{01}=0.25\times10^{-16}$ cm^2 for 1 keV, 0.7×10^{-16} cm^2 for 2 keV, 0.85×10^{-16} cm^2 for 5 keV, and 0.9×10^{-16} cm^2 for 10 keV (Refs. 10 and 12). (See also Ref. 11.)

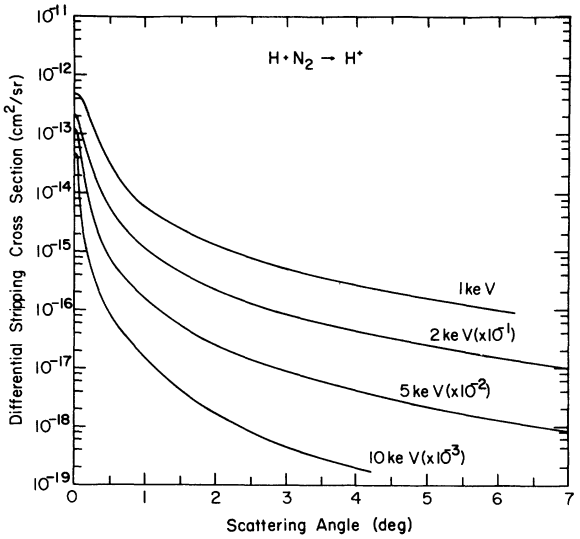

FIG. 10. Differential stripping cross sections for molecular nitrogen. Assumed total cross sections $\sigma_{01} = 0.7\times10^{-16}$ cm^2 for 1 keV, 1.25×10^{-16} cm^2 for 2 keV, 2.2×10^{-16} cm^2 for 5 keV, and 3.4×10^{-16} cm^2 for 10 keV (Ref. 10). (See also Ref. 11.)

sions of fast neutrals with target-gas atoms or molecules directly in front of the detector aperture. In spite of the much smaller target-gas density in this region as compared with the density in the collision cell, these contributions can become quite significant for small scattering angles when the detector is positioned close to the original neutral beam. (Ions resulting from collisions have a rather large probability of passing through the detector aperture owing to the closeness of the detector aperture.) This effect was tested by partially closing the gate valve in front of the diffusion pump connected to the rotatable chamber, and thus artificially raising the target-gas pressure in this region relative to that in the small collision cell itself. From the results it appeared that collisions of this type could contribute as much as 30–40% of the small-angle signal when the small diffusion pump and the two extra apertures in front of the detector were removed. After their insertion, these contributions were negligible.

In separate tests, the angular distribution of the protons was determined vertically by moving both detector sleds equal steps in the vertical direction. In Fig. 4, results of these measurements are compared with a usual horizontal distribution. The two distributions agree very well. From optical alignment checks, it was found that the small apparent deviation around 0.8°, probably was due to the beginning of a geometric cutoff of the beam by the upper rim of the exit aperture of the collision cell. The good agreement between these two scans is another indication that the measured distributions were not seriously disturbed by electric or magnetic stray fields between the collision cell and the detector.

To test the influence of the beam resolution on the measured distributions, some measurements were performed using the wide aperture set at higher beam energies. An example of this is shown in Fig. 5 in which angular distributions measured

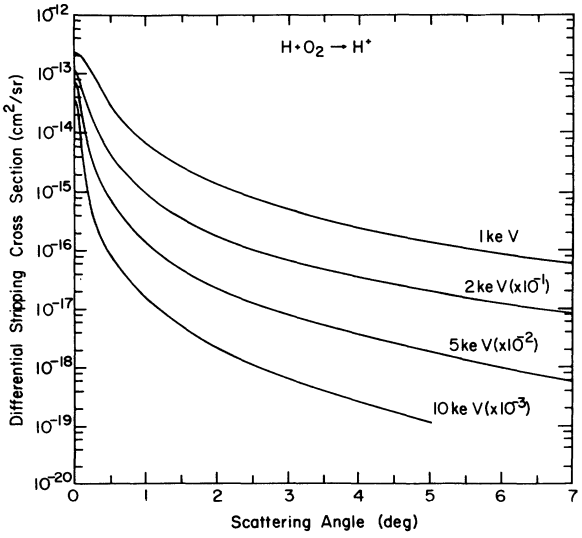

FIG. 11. Differential stripping cross sections for molecular oxygen. Assumed total cross sections $\sigma_{01} = 0.55\times10^{-16}$ cm^2 for 1 keV, 0.9×10^{-16}cm^2 for 2 keV, 2.0×10^{-16} cm^2 for 5 keV, and 3.3×10^{-16} cm^2 for 10 keV (Ref. 12). (See also Ref. 11.)

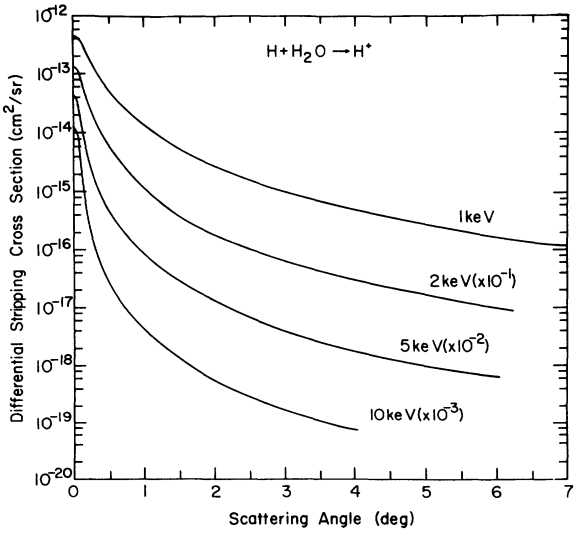

FIG. 12. Differential stripping cross sections for water vapor. For all energies, a total cross section $\sigma_{01} = 1\times10^{-16}$ cm^2 is assumed. (See also Ref. 11.)

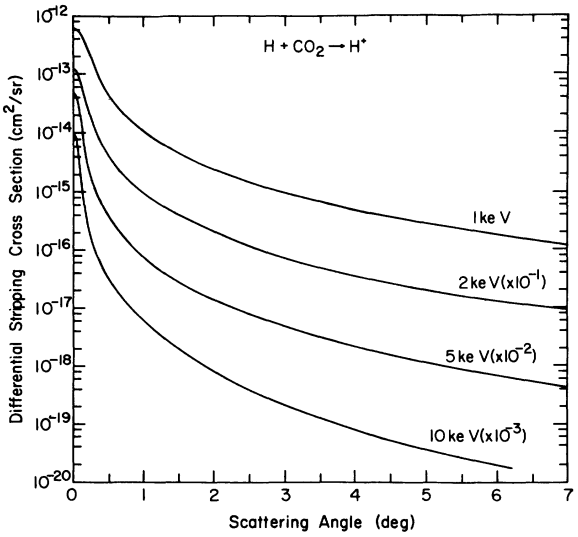

FIG. 13. Differential stripping cross sections for carbon dioxide. For all energies, a total cross section $\sigma_{01} = 1 \times 10^{-16}$ cm^2 is assumed (See also Ref. 11.)

with the wide and the narrow aperture sets are compared for the case of 5-keV beam energy and nitrogen as target gas. In this plot, the large-angle data are normalized to the same intensity. Also the original neutral-beam distributions are shown. No correction of the measured distributions for beam resolution were performed, and in the following, all data are plotted directly as obtained. Over-all, we expect that these distributions are correct within about 15% rms in intensity or about 0.02° rms in angle. From such measurements, it appears that for the combination of apertures and beam energies used in the final measurements the influence of beam resolution can be practically neglected for all measurements at 1 and 2 keV and for most measurements at 5 keV (excepting the very narrow distributions for H_2 and He). For all other measurements, these corrections certainly fall within the remaining experimental accuracy for all scattering angles larger than 0.2°–0.3°.

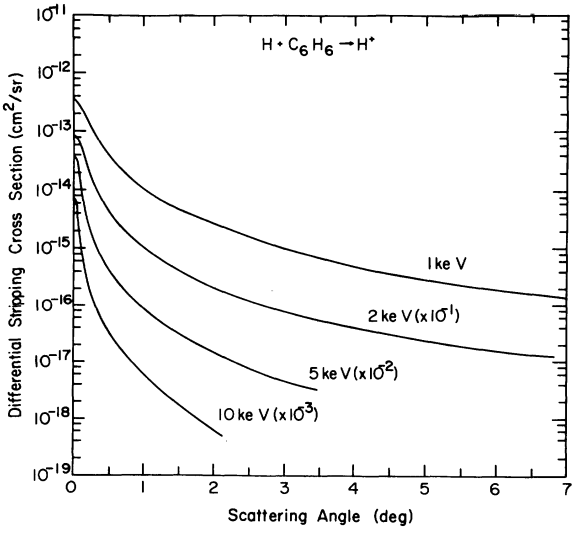

FIG. 14. Differential stripping cross sections for benzene vapor. For all energies, a total cross section of $\sigma_{01} = 1 \times 10^{-16}$ cm^2 is assumed. (See also Ref. 11.)

The size of possible influences on our distributions from multiple scattering of the ions in the stripping cell was tested in a variety of cases by measuring the angular distributions at two different gas pressures. Since such effects, if at all, would be most prominent in the forward direction, one of these gas pressures was always in the "low-pressure" regime mentioned above, the other clearly above. The ratio between the pressures used was 2–3 and higher. In all cases the two distributions agreed to within the quoted general uncertainties.

IV. RESULTS AND DISCUSSION

The resulting distributions are plotted in Figs. 6–14 in the form of angularly differential cross section $d\sigma/d\Omega(\theta)$. (A tabular presentation of the same data can be found in Ref. 11.) The absolute calibration for these cross sections was obtained by integrating the partially measured angular distribution $f(\theta)$,

$$I = \int_0^{2\pi} f(\theta) \sin\theta \, d\theta$$

and comparing this integral with the total cross section σ_{01} for stripping of the hydrogen atoms in the respective gas, i.e., by writing

$$\sigma_{01} = \alpha I,$$

with the calibration constant α, so that

$$\frac{d\sigma}{d\Omega(\theta)} = \alpha f(\theta).$$

In these integrals, the contributions from angles larger than those measured was estimated by a logarithmic extrapolation of the measured curves. For energies $E \geq 2$ keV these contributions generally were smaller than about 10% so that an overall integration error of 5–10% may be expected. For $E = 1$ keV, in particular, for the heavier gases, contributions of up to 20% were estimated. Correspondingly, the integration errors may be sizable in these cases.

The total cross-section values from Refs. 12–14 used in this conversion are exhibited in Table I for all energies and gases. The cross sections

TABLE I. Total stripping cross sections σ_{01} on which normalization of differential cross sections is based. All cross sections in units of 10^{-16} cm^2.

Energy (keV)	He	Ar	Kr	H_2	N_2	O_2	H_2O	CO_2	C_6H_6
1	0.3	0.3	0.3	0.25	0.7	0.55	1.0	1.0	1.0
2	0.6	0.6	0.7	0.7	1.25	0.9	1.0	1.0	1.0
5	1.2	1.3	1.55	0.85	2.2	2.0	1.0	1.0	1.0
10	1.4	2.1	3.0	0.9	3.4	3.3	1.0	1.0	1.0
Refs.	12,13	12,13 14	13,14	10,12	12	12	assumed	assumed	assumed

for the rare gases and the diatomic gases pertaining to energies $E \geq 2$ keV were obtained as weighted averages from the references given in the table. The cross sections for the same gases and 1-keV beam energy were derived by extrapolation of the same curves. No reliable total stripping cross sections could be found for the remaining gases, CO_2, H_2O, and C_6H_6. Therefore, the respective differential cross sections in Figs. 12–14 are all normalized to an assumed total cross section of 1×10^{-16} cm^2.

The errors on the measured total cross sections reported in these references are hard to estimate. In general, we would expect an uncertainty of 20%, and thus, an uncertainty of about 30% for the presented absolute values of our differential cross sections.

All curves plotted in Figs. 6–14 show a monotonic decrease of the differential stripping cross section with increasing angle. No particular structure attributable to curve-crossing effects or similar effects is apparent even for the case of $H+H_2$, where the energy dependence of the total stripping cross section[10] exhibits a slight structure. It seems that in all these collisions the stripping process is dominated by a pure knock-on ionization. Also, for a given energy, the distribution widths do not vary greatly with target gas. As an example, Figs. 15(a) and 15(b) show renormalized angular distributions for a beam energy of 2 keV and various target gases. Only the lightest target gases, H_2 and He, exhibit a relatively narrow distribution of the stripped protons. The distributions of all other gases are quite similar in width and behavior.

The dependence of the angular distributions on the beam energy is approximately as expected. The width of the distributions decreases with energy, roughly proportional to $1/E$. This is particularly evident from Fig. 16, which shows, as a function of energy, the half-cone-angles θ_{50} and θ_{75} into which 50% and 75%, respectively, of the total number of stripped protons is scattered. These points were obtained by the mentioned integration process, and therefore, contain the mentioned extrapolation errors. We estimate that the 50% angles are correct within about 5–10% for beam energies $E \geq 2$ keV, probably including the strong scatterers Kr and C_6H_6. For 1 keV, this limit may have to be raised to 15%. For the 75% angles, the uncertainties certainly are larger, probably roughly 5–10% for $E \geq 5$ keV, 10–15% for 2 keV, and up to 20% for 1 keV. In particular, the upper error limits seem appropriate for the strongly scattering gases, Kr and C_6H_6.

It appears that the product of these scattering angles, θ_{50} and θ_{75}, with the beam energy is more or less independent of the energy for the measured multiatomic gases. The good agreement of the values of about 1 keV deg for nitrogen and oxygen with a cutoff scattering angle of 15° at 100-eV beam energy inferred earlier[15] from more integral measurements may indicate that roughly the same $E\theta_{50}$ values still hold down to 100 eV.

For monatomic gases the values of this product may increase slightly at smaller energies. Again, this would be consistent with the relatively faster increase of the detector efficiency with beam energies found in Ref. 15 when argon is used as stripping gas. The apparent comparative increase of the 50% angles in He and H_2 at 10 keV probably is not real but is mostly a result of the finite angular resolution in our measurements which tends to raise these points more at larger energies, where the actual scattering angles are smallest.

From these integrated scattering angles, error estimates for earlier measurements of total stripping cross sections for hydrogen atoms in various gases can be deduced. Such measurements were reported by various groups (Refs. 10, 12–14, and 16–18). In all of these papers, very little information is given concerning the maximum scattering angle of the resulting protons accepted by the final detector. Only McClure[10] has made good determination of the scattering. Of the others, it appears that the smallest errors may have resulted in the measurements of Stier and Barnett,[12] since the absorption technique used in

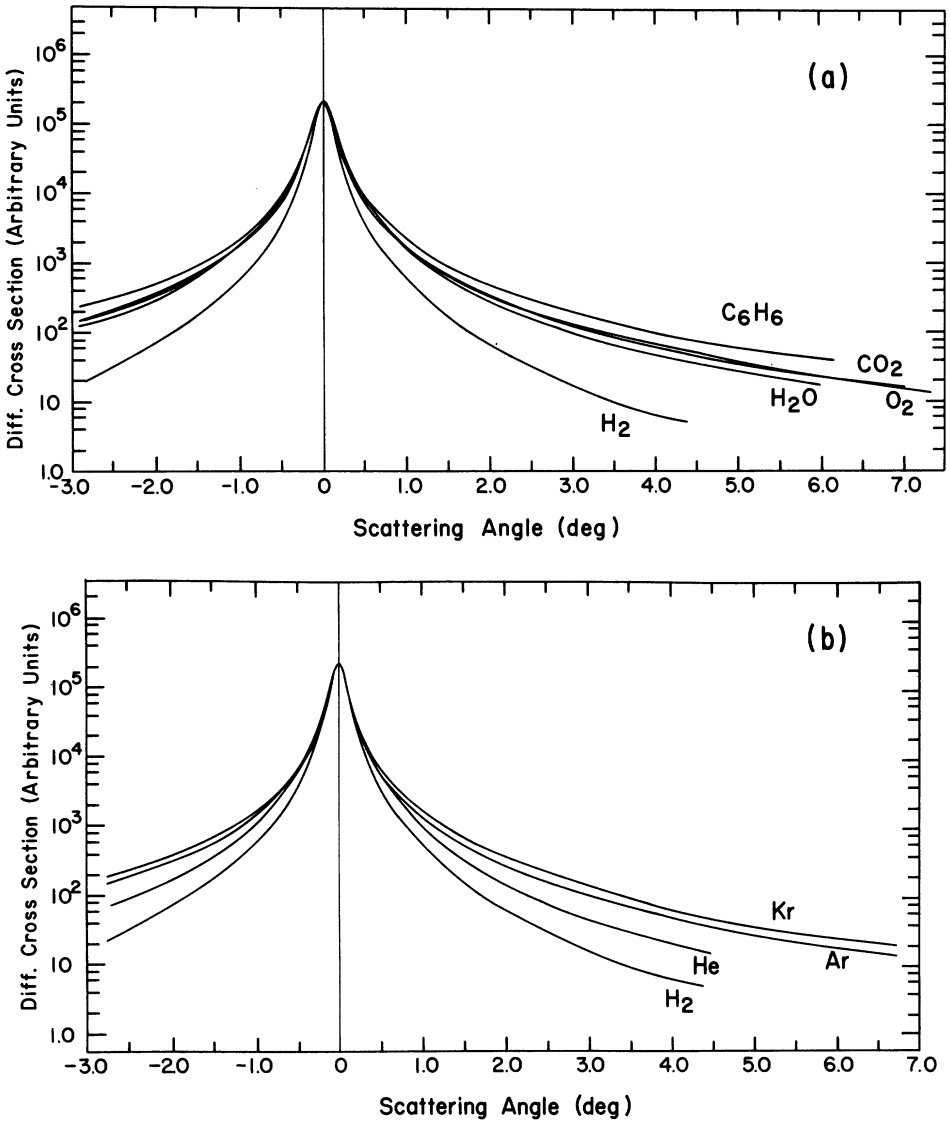

FIG. 15. (a) Comparison of angular distributions at 2 keV for various target gases. (b) Comparison of angular distributions at 2 keV for various target gases.

these measurements is least sensitive to such scattering. In the measurements of Williams,[13] acceptance angles of about 0.5°–1° were used.[19] Thus, the scattering losses even at the lowest energy, 2 keV, generally may have been negligible for the lightest target gases, H_2 and He. However, these errors may have amounted up to 50% for the heavier target gases at low beam energies. In the case of the Russian group, again no exact data on the maximum acceptance angle are available. However, from the dimensions given in Fig. 1 and the adjacent text of Ref. 16, it appears that this angle probably was not more than 0.3°–0.4°. Thus, scattering losses may have reduced the measured cross sections by a factor of almost 2 for the heavier target gases and the lowest beam energies, 5 keV. The experimental checks mentioned in Ref. 16 were made only at beam energies of 15 and 30 keV, where the scattering losses indeed become negligible.

For further analysis, the differential cross sections for the atomic gases He, Ar, and Kr are replotted in Figs. 17–19 in the normalized form described by Smith *et al.*,[20] i.e., $\rho = \theta \sin\theta \, d\sigma/d\Omega$ is plotted as a function of the normalized scattering angle $\tau = E\theta$. In this normalized form, all elastic scattering distributions for a charged particle and a given velocity-independent interaction potential would fall on a general curve which is determined only by this interaction po-

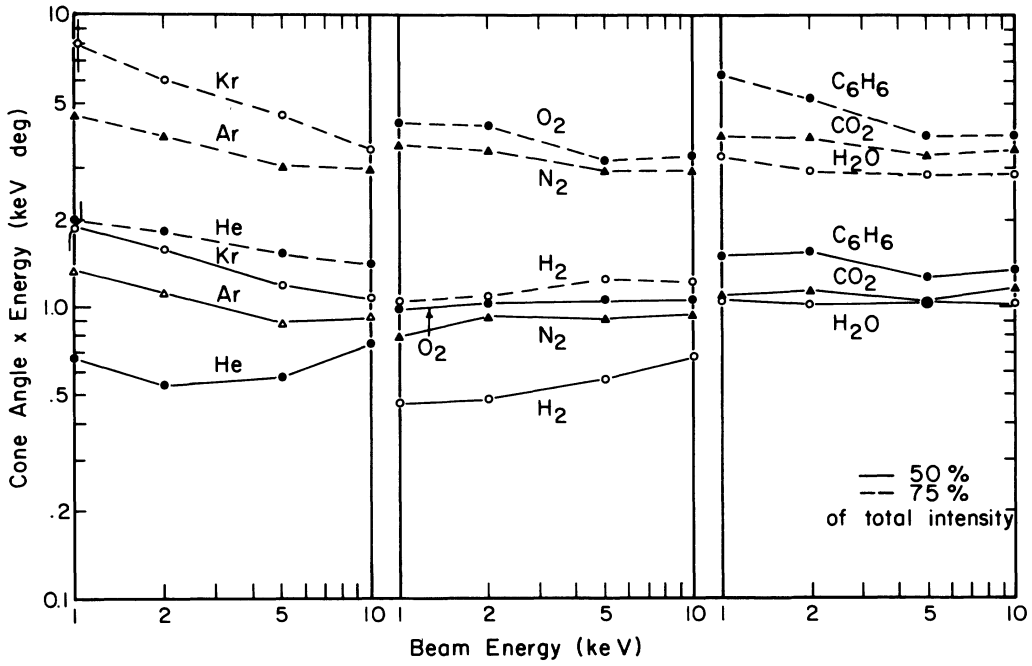

FIG. 16. Cone half-angles into which 50 to 75% of the total intensity of resulting protons are scattered.

tential, and each $E\theta$ value then belongs to a certain value of the collisional impact parameter b.

For all three gases, the curves for various energies are parallel to each other at large values of $E\theta$ within the mentioned experimental errors. At smaller $E\theta$ values, the high-energy curves exhibit an additional bulge. However, these bulges appear to be due mainly to the finite beam resolution. The vertical lines attached to each curve are drawn at an angle twice the geometric beam resolution determined earlier. At angles somewhat smaller than this value, the beam resolution provides for an apparent exaggeration of the measured cross sections; towards even smaller

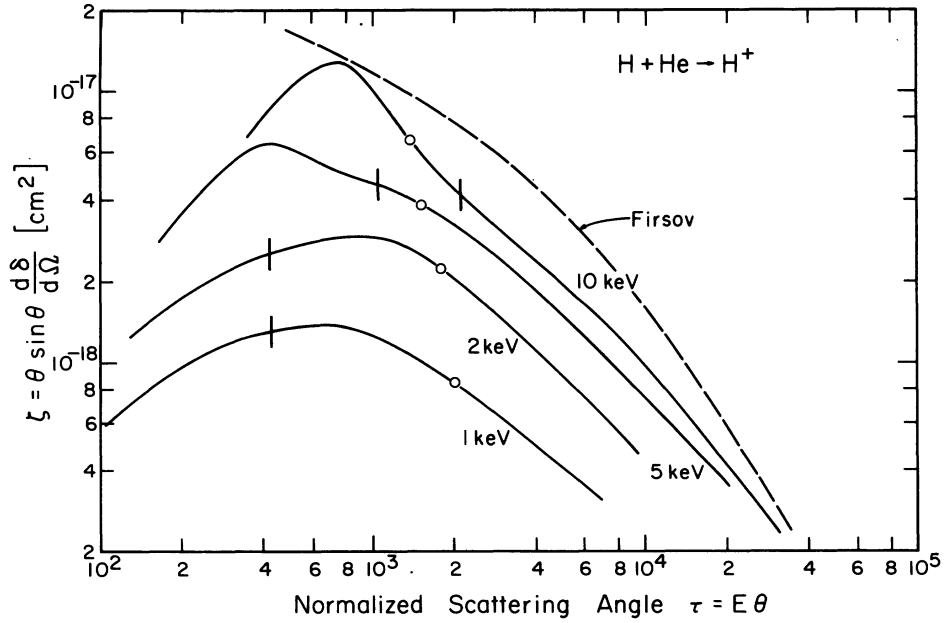

FIG. 17. Normalized plot of differential stripping cross sections in He. "Firsov": scattering from shielded Coulomb potential (1a) and (1b). (□ 50%-angle, ○ 75%-angle, vertical-line beam resolution.)

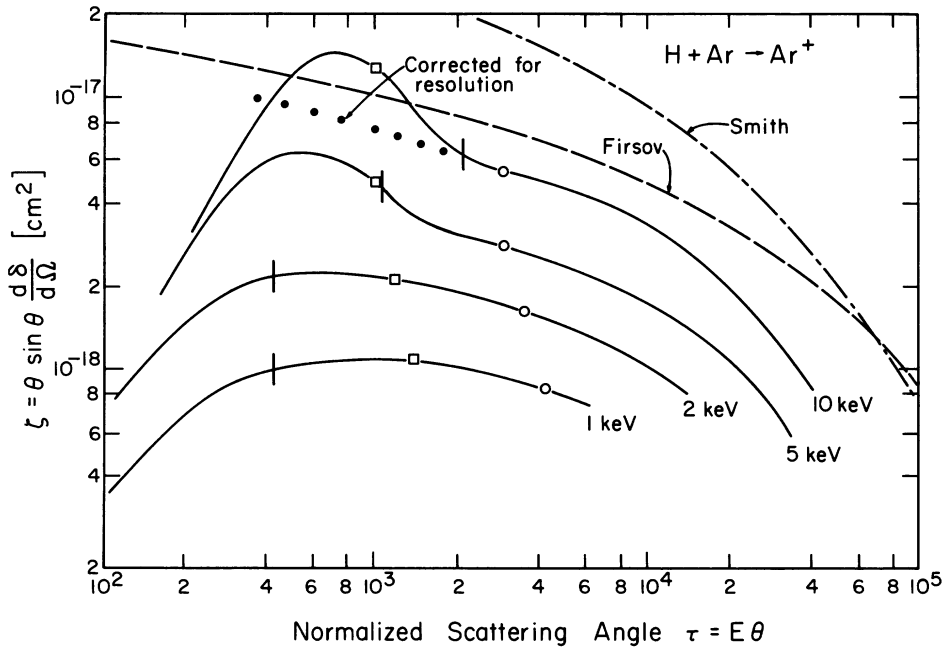

FIG. 18. Normalized plot of differential stripping cross sections in Ar. "Firsov": scattering from shielded Coulomb potential (1a) and (1b). "Smith": scattering from shielded Coulomb potential using $c = 0.8\, a_0$. (□ 50%-angle, ○ 75%-angle, vertical-line beam resolution.)

scattering angles, the seeming linear decay of the measured normalized cross section results. A rough correction of the 10-keV curves taking into account the measured beam geometry indicates a continuous extension of the real normalized cross section into this small-angle regime, as indicated by the dotted line in Fig. 18. The measured bulge thus becomes only a measure of the total intensity of protons at small angles. However, for beam energies of 1–2 keV a faster decay of the actual differential cross section at small angles seems to exist.

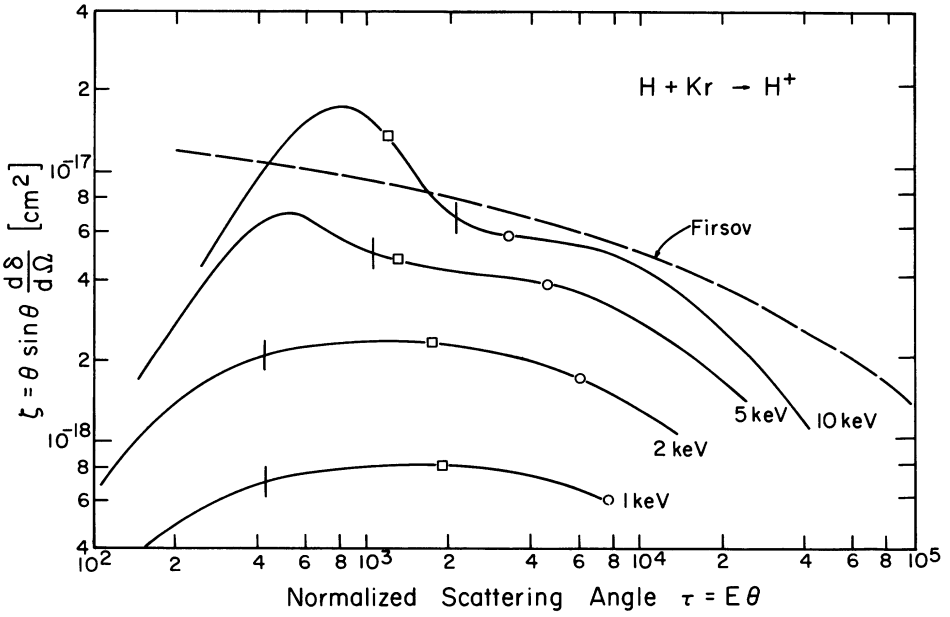

FIG. 19. Normalized plot of differential stripping cross sections in Kr. "Firsov": scattering from shielded Coulomb potential (1a) and (1b). (□ 50%-angle, ○ 75%-angle, vertical-line beam resolution.)

Thus, the actual normalized-cross-section curves for these three gases appear to be parallel over a wide range of normalized angles with the absolute values being roughly proportional to the total cross sections. The same holds true also for the measured molecular target gases. Only at small $E\theta$ values, i.e., at large impact parameters, do the actual cross sections seem to decrease faster at low beam energies than at 10 keV. This fact indicates that the logarithm of the stripping probability P_{01} increases uniformly with energy E for all impact parameters b below a certain energy-dependent "cutoff distance," i.e., the stripping probability $P_{01}(b,E) = B(b)p(E)$ is the product of two independent functions of the impact parameter and the beam energy in this range. The limiting cutoff distance seems to increase with the energy.

A more detailed experimental investigation of $P_{01}(\theta, E)$ will be contained in a subsequent paper.[21] In the following, we will compare only the shape of the normalized curves with the normalized curve for the scattering of a heavy particle from an exponentially screened Coulomb potential,

$$V(r) = (Z_t e^2/4\pi\epsilon_0 r)e^{-r/c} \tag{1a}$$

(Z_t is the atomic number of the target, c is the shielding distance) as analyzed in Ref. 20. The dashed curves in Figs. 17–19 give the result for a shielding distance

$$c = 0.885a_0/(1+z_t^{2/3})^{1/2} \tag{1b}$$

as it was projected by Firsov[22] for the interaction between a hydrogen atom and a target atom with atomic number Z_t and was used in a similar elastic scattering analysis by Smith *et al.*[23] for He^+ on Ar.

For He and Ar as targets these theoretical curves are almost parallel to the measured distributions indicating only slow changes of the stripping probability P_{01} with impact parameter. Using the same theoretical interaction potentials and normalized scattering curves, the impact parameters b_{50} and b_{75} which correspond to the mentioned angles θ_{50} and θ_{75}, respectively, can be estimated. Table II gives a summary of the results derived according to Ref. 20.

TABLE II. Estimated impact parameter for scattering angles θ_{50} and θ_{75} for screened Coulomb potential (1) in He and Ar.

	Energy (keV)	b_{50} (Å)	b_{75} (Å)
He	1	scattering	0.40
	2	angles	0.42
	5	below	0.44
	10	resolution	0.47
Ar	1	0.65	0.47
	2	0.67	0.50
	5	0.70	0.52
	10	0.70	0.53

The theoretical scattering curve and the resulting impact parameters of Table II depend on the screening length c. For the elastic scattering of He^+ from Ar, Smith *et al.*[23] derived a more optimal effective screening length $c_{Ar} = 0.8a_0$. If this length is used for argon, the dash-dotted curve in Fig. 18 results, which is very nearly parallel to our measured curves. In this case the respective inferred impact parameters of Table II approximately double. A more detailed analysis of the results of a direct measurement of the stripping probability P_{01} will be reported in Ref. 21.

For Kr, the theoretical curve of Fig. 19 deviates from the measured distributions more seriously at large $E\theta$ values. Therefore, no similar estimate is tried in this case.

The observed parallelism of the various nor-

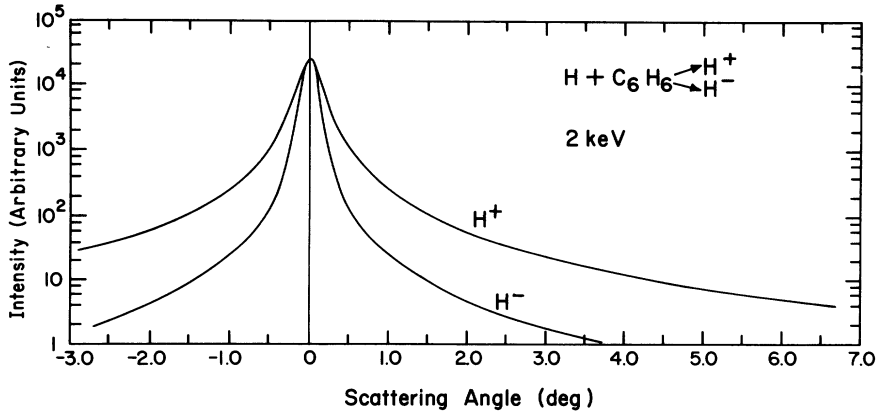

FIG. 20. Comparison of angular distributions of H^+ and H^- resulting from $H + C_6H_6$ collisions.

malized angular distributions for each target gas agrees very well with a similar finding for the stripping of He on He in Ref. 7. Also, the more recent stripping results on the system Ar + Ar by Eriksen *et al.*[24] show a similar behavior when they are replotted in this normalized form. However, in contrast to the strong forward peaking of our angular distributions a pronounced minimum of the resulting ion distribution in the forward direction followed by a distribution maximum at a normalized angle of $E\theta_{max} = 6000$ eV deg is reported in this later case.

Such a dip in forward direction followed by a maximum, the position of which scales with $1/E$, has been observed for reactions which are understood to proceed through crossings of the respective molecular-potential curves, as in the case of $He^+ + Ar \rightarrow He + Ar^+$ (see Ref. 25). On the other hand, reactions which exhibit a "Massey maximum,"[26] as the charge-transfer reaction $H^+ + O_2 \rightarrow H + O_2^+$, have been found[27] to exhibit a pronounced peak in the forward direction. The difference in the forward scattering of the reaction products Ar^+ and H^+ correlates well with the different scaling characteristics of the total cross sections for these two stripping reactions pointed out in Ref. 4. At that time, it was observed that the reaction $Ar + Ar \rightarrow Ar^+ + Ar$ is well described by Firsov's model,[3] and this is equally true for the total cross section for total electron production in Ar + Ar collisions as measured by Amme and Hayden.[28] On the other hand, the stripping of H atoms in gases appeared to be described better by a direct transition model. It appears that the minimum in forward direction of the angular distribution is directly connected with the existence of the critical impact parameter R_c in Firsov's theory beyond which no reaction takes place, whereas in direct reactions generally no such dip is found.

In addition to the described stripping measurements, a few angular distributions of H^- ions resulting from collisions of the neutral H atoms with the target gases were measured. It was found that these distributions generally are narrower than those of the H^+ ions from the corresponding stripping reactions. An example of the results is shown in Fig. 20.

---

*This work was supported by the U. S. Atomic Energy Commission, and in part by the National Science Foundation.

[1]A complete list of all experimental data published between 1950 and 1970 can be found in R. C. Dehmel, H. K. Chau, and H. H. Fleischmann, At. Data 5, 231 (1973).

[2]A. Russek and M. T. Thomas, Phys. Rev. 109, 2015 (1958); 114, 1538 (1959); A. Russek, Phys. Rev. 132, 246 (1963); Physica 48, 165 (1970).

[3]O. B. Firsov, Zh. Eksp. Teor. Fiz. 36, 1517 (1959) [Sov. Phys.—JETP 9, 1076 (1959)].

[4]H. H. Fleischmann, R. C. Dehmel, and S. K. Lee, Phys. Rev. A 5, 1784 (1972).

[5]D. M. Kaminker and N. V. Fedorenko, Zh. Tekhn. Fiz. 1, 1843 (1955).

[6]W. J. Savola, Jr., F. J. Eriksen, and E. Pollack, in Proceedings of the 23rd Annual Gaseous Electronic Conference, Hartford, 1970 (unpublished).

[7]R. Francois, D. Duicq, and M. Barat, in Proceedings of the Seventh International Conference on Electronic and Atomic Collisions, Amsterdam, 1971.

[8]See, for instance, P. R. Jones, F. P. Ziemba, H. A. Moses, and E. Everhart, Phys. Rev. 113, 182 (1959); or, more recently, W. C. Keever, G. J. Lockwood, H. F. Helbig, and E. Everhart, Phys. Rev. 166, 68 (1966); and E. J. Knystautas, Q. C. Kessel, R. DelBoca, H. C. Hayden, Phys. Rev. A 1, 825 (1970).

[9]L. I. Pivovar, M. T. Novikov, and A. S. Dolgov, Zh. Eksp. Teor. Fiz. 49, 734 (1965); 50, 537 (1966) [Sov. Phys.—JETP 22, 508 (1966); 23, 357 (1966)].

[10]G. W. McClure, Phys. Rev. 166, 22 (1968).

[11]A. Complete tabular presentation of all experimental results can be obtained from ASIS/NAPS, c/o Microfiche Publications, 305 E. 46th Street, New York, N.Y. 10017 (NAPS document No. 02380 for 9 pages). Remit with order for each NAPS document number $1.50 for microfiche or $5.00 for photocopies. Make checks payable to "Microfiche Publications."

[12]P. M. Stier and C. F. Barnett, Phys. Rev. 103, 896 (1956).

[13]J. F. Williams, Phys. Rev. 153, 116 (1967).

[14]E. S. Soloviev, R. N. Ilin, V. A. Oparin, and N. V. Fedorenko, Zh. Eksp. Teor. Fiz. 42, 659 (1962) [Sov. Phys.—JETP 15, 459 (1962)].

[15]H. H. Fleischmann, and R. T. Tuckfield, Nucl. Fusion 8, 81 (1968).

[16]Ya. M. Fogel', V. A. Ankudinov, D. V. Pilipenko, and N. V. Topolia, Zh. Eksp. Teor. Fiz. 34, 579 (1958) [Sov. Phys.—JETP 7, 400 (1958)].

[17]Ya. M. Fogel', V. A. Ankudinov, and D. V. Pilipenko, Zh. Eksp. Teor. Fiz. 38, 26 (1960) [Sov. Phys.—JETP 11, 18 (1960)].

[18]D. V. Pilipenko, and Ya. M. Fogel', Zh. Eksp. Teor. Fiz. 42, 936 (1962); 44, 1818 (1963) [Sov. Phys.—JETP 15, 646 (1962); 17, 1222 (1963)].

[19]J. F. Williams (private communication).

[20]F. T. Smith, R. P. Marchi, and K. G. Dedrick, Phys. Rev. 150, 79 (1966).

[21]C. F. Barnett (unpublished).

[22]O. B. Firsov, Zh. Eksp. Teor. Fiz. 34, 447 (1958) [Sov. Phys.—JETP 7, 308 (1958)].

[23]F. T. Smith, R. P. Marchi, W. Aberth, and D. C. Lorents, Phys. Rev. 161, 31 (1967).

[24]F. J. Eriksen, S. M. Fernandez, A. V. Bray, and E. Pollak, in The Third International Conference on

Atomic Physics, Boulder, Colorado, 1972, p. 70 (unpublished).
[25]F. T. Smith, H. H. Fleischmann, and R. A. Young, Phys. Rev. A 2, 379 (1970).
[26]H. S. W. Maney, Rep. Prog. Phys. 12, 248 (1948).
[27]H. H. Fleischmann, R. A. Young, and J. W. McGowan, Phys. Rev. 153, 19 (1967).
[28]R. C. Amme and H. C. Hayden, J. Chem. Phys. 44, 2828 (1966).